

# Plasmon modes and negative refraction in metal nanowire composites

Viktor A. Podolskiy

*Electrical Engineering Department, Princeton University, Princeton,  
NJ 08544*

[vpodolsk@princeton.edu](mailto:vpodolsk@princeton.edu)

<http://corall.ee.princeton.edu/vpodolsk>

Andrey K. Sarychev and Vladimir M. Shalaev

*School of Electrical & Computer Engineering, Purdue University,  
West Lafayette, IN 47907*

[sarychev@ecn.purdue.edu](mailto:sarychev@ecn.purdue.edu) [shalaev@purdue.edu](mailto:shalaev@purdue.edu)

**Abstract:** Optical properties of metal nanowires and nanowire composite materials are studied. An incident electromagnetic wave can effectively couple to the propagating surface plasmon polariton (SPP) modes in metal nanowires resulting in very large local fields. The excited SPP modes depend on the structure of nanowires and their orientation with respect to incident radiation. A nanowire percolation composite is shown to have a broadband spectrum of localized plasmon modes. We also show that a composite of nanowires arranged into parallel pairs can act as a left-handed material with the effective magnetic permeability and dielectric permittivity both negative in the visible and near-infrared spectral ranges.

© 2003 Optical Society of America

**OCIS codes:** (160.4670) Optical materials; (260.5740) Physical Optics, resonance; (310.6860) Thin films, optical properties

---

## References and links

1. S. D. M. Brown, P. Corio, A. Marucci, M. A. Pimenta, M. S. Dresselhaus, and G. Dresselhaus, "Second-order resonant Raman spectra of single-walled carbon nanotubes," *Phys. Rev. B* **61**, 7734-7742 (2000);
2. K. B. Shelimov, and M. Moskovits, "Composite Nanostructures Based on Template-Grown Boron Nitride Nanotubules," *Chemistry of Materials*, **12**, 250 (2000);
3. J. Li, C. Papadopoulos, J.M. Xu, and M. Moskovits, "Highly-ordered carbon nanotube arrays for electronics applications," *Applied Physics Letters* **75**, 367 (1999);
4. J.B. Pendry, "Negative Refraction Makes a Perfect Lens," *Phys. Rev. Lett.* **85**, 3966 (2000);
5. V. G. Veselago, "The electrodynamics of substances with simultaneously negative values of  $\epsilon$  and  $\mu$ ," *Soviet Physics Uspekhi* **10**, 509 (1968).
6. D.R. Smith, W.J. Padilla, D.C. Vier, S.C. Nemat-Nasser, S. Shultz, "Composite Medium with Simultaneously Negative Permeability and Permittivity," *Phys. Rev. Lett.* **84**, 4184 (2000);
7. G.Shvets, "Photonic approach to making a material with a negative index of refraction," *Phys.Rev.B* **67**, 035109 (2003)
8. V.A.Podolskiy, A.K. Sarychev, and V.M. Shalaev, "Plasmon modes in metal nanowires and left-handed materials," *Journal of Nonlinear Optical Physics and Materials* **11**, 65 (2002)
9. L.V.Panina, A.N.Grigorenko, D.P.Makhnovskiy, "Optomagnetic composite medium with conducting nanoelements," *Phys.Rev.B* **66**, 155411 (2002)

10. E.M.Purcell and C.R.Pennypacker, "Scattering and absorption of light by nonspherical dielectric grains," *Astrophysical Journal* **186**, 705 (1973)
  11. J.D. Jackson *Classical Electrodynamics*, (J.Wiley&Sons, Inc, 1999)
  12. B.T.Draine, "Discrete dipole approximation and its application to interstellar graphite grains," *Astrophys.J.* **333**, 848 (1988)
  13. V.A. Markel, "Antisymmetrical optical states," *J.Opt.Soc.Am.* **B12** 1783 (1995)
  14. V.A.Markel, "Scattering of light from two interacting spherical particles," *J.Mod.Opt* **39** 853 (1992)
  15. B.T.Draine "The discrete dipole approximation for light scattering by irregular targets" in *Light Scattering by Nonspherical Particles: Theory, Measurements, and Applications*, Acad.Press (2000)
  16. M. Moskovits, private communication
  17. N.Yamamoto, K.Araya, M.Nakano, F.J.Garsia de Abajo, "Direct imaging of plasmons in nanostructures", annual OSA meeting 2002, Orlando, Florida
  18. D.Stauffer and A.Aharony *Introduction to percolation theory*, (Taylor and Fransis, 1994)
  19. S.Ducourtieux, et al, "Near-field optical studies of semicontinuous metal films," *Phys.Rev.B* **64** 165403 (2001)
  20. V. M. Shalaev (editor) *Optical Properties of Nanostructured Random Media* , Topics in Applied Physics, v. 82, (Springer Verlag, Berlin, 2002)
  21. A.N. Lagarkov and A.K. Sarychev, "Electromagnetic properties of composites containing elongated conducting inclusions," *Phys.Rev.B* **53**, 6318 (1996)
- 

## 1. Introduction

The optical properties of nanostructured materials have been intensively studied during the last decade (see, for example, [1, 2, 3]). Various "nano" versions of major optics areas, such as nanophotonics and nanospectroscopy, are developing with increasing rate. Among particularly important problems in this field is the focusing and guiding of light on nanometer scales beyond the diffraction limit of conventional far-zone optics.

For object imaging, the near-field part of the radiation contains all the information about the scatterer. As the distance from the object increases, the evanescent portion of the scattered field exponentially decays, resulting in loss of information on the "fine" (sub-wavelength) features of the scatterer. The usual way to solve this problem is to use shorter wavelengths or measure in the near-zone; both of these methods have their limitations. A new way to solve this imaging problem has been recently proposed by Pendry [4] (see also [5]). According to Pendry, when the scattered light passes through a material with negative refractive index (specifically, it should be equal to -1), the evanescent components of the scattered field are enhanced allowing the restoration of the object image with subwavelength resolution. Despite the obvious importance of such super-lens, it is worth noting here that possible applications for materials with negative refraction can go far beyond this idea. This is because the refractive index enters into most optical "laws" so that the possibility of its sign reversal can result in their serious revision and new applications resulting from this.

Smith *et al.* [6] have demonstrated negative-refraction materials (also referred to as left-handed materials, LHMs, because the electric, magnetic vectors and the wavevector form a left-handed system, in this case) in the microwave range. Shvets proposed how such "meta-materials" can be made in the far-IR part of the spectrum [7]. In our previous paper [8], we proposed a first LHM (based on a nanowire composite) that can have negative refraction in the near-IR and visible spectral ranges. A similar nanowire system was later considered by Panina *et al.* [9].

In the present paper we study the optical properties of metal nanowires and their various composites. We verify our previous theoretical results (limited by the approximation used in [8]) with new numerical simulations and study the behavior of nanowire plasmon modes in more detail. We show that metal nanowires and their composites can act as nano-resonators capable of producing the local-field enhancement up to  $10^3$ . We

also describe how nanowire composites can be used for developing LHMs *in the near-IR and visible* parts of the spectrum.

The rest of the paper is organized as follows. In the next Section we present the numerical method used to find the electromagnetic field distribution for metal nanowires. In Section 3, we consider the optical response of a single nanowire and verify the existence of surface plasmon polariton (SPP) resonance in such a system. We show here that the local field near a metal nanowire can be dramatically enhanced due to such resonance. When nanowires form a percolation composite, the interactions between the nanowires result in many localized plasmon modes, with different resonant frequencies that all together cover a very large spectral range. In Section 4 we show that the forward and back-scattering by the nanowire system can be characterized by their effective dipole and magnetic moments. The last Section of our paper considers composite materials based on parallel pairs of nanowires. We show here that both electrical and magnetic resonances can occur in such material and, under certain conditions, it can have a negative refractive index. We numerically study here the resonant properties of nanowire pairs as functions of different parameters.

## 2. Coupled Dipole Equations (CDEs)

We start by briefly recapitulating our previous results [8] on the optical properties of a single nanowire. These properties are governed by two important nanowire dimensions, the diameter and length. The radius of the wire,  $b_2$ , we assume to be much smaller than the wavelength of the incident light,  $\lambda$ ; the radius, however, can be comparable with the optical skin-depth in the metal. The length of the nanowire,  $2b_1$ , can be on the order of light wavelength. Such relations between parameters of the system makes it very hard to solve the Maxwell equations exactly; they can be, however, analyzed numerically.

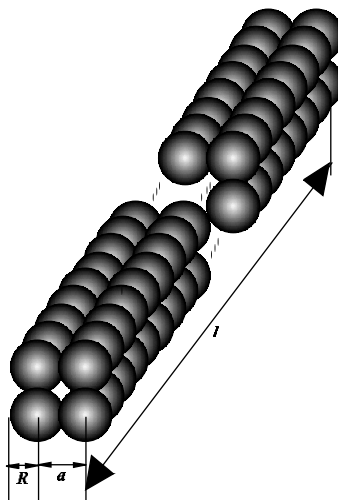


Fig. 1. A nanowire represented by an array of “intersecting” spheres [8]

To find numerical solution to the Maxwell equations for our system we use the discrete-dipole approximation (DDA). This approach was first introduced by Purcell and Pennypacker [10] to find the scattering properties of irregularly-shaped objects. In this method, an object is replaced by a large number ( $N$ ) of interacting polarizable spheres placed on a cubic lattice (see Fig. 1). The lattice period  $a$  (and thus the radius of individual spheres,  $R$ ) is much smaller than the wavelength of the incident light. If the relation  $a \ll \lambda$  is fulfilled, then each dipole can be treated in the quasi-static

approximation with the field given by the sum of the incident field and the fields due to all other dipoles, as described by the following coupled-dipole equations (CDEs)

$$\mathbf{d}_i = \alpha_0 \left[ \mathbf{E}_{inc} + \sum_{j \neq i}^N \hat{G}(\mathbf{r}_i - \mathbf{r}_j) \mathbf{d}_j \right], \quad (1)$$

where  $E_{inc}$  represents the incident field at the location of the  $i$ -th dipole,  $\mathbf{r}_i$ ,  $\hat{G}(\mathbf{r}_i - \mathbf{r}_j) \mathbf{d}_j$  represents the EM field scattered by dipole  $j$  at this point, with  $\hat{G}$  being a regular part of the free-space dyadic Green function. The latter is defined as

$$\begin{aligned} G_{\alpha\beta} &= k^3 [A(kr) \delta_{\alpha\beta} + B(kr) r_\alpha r_\beta], \\ A(x) &= [x^{-1} + ix^{-2} - x^{-3}] \exp(ix), \\ B(x) &= [-x^{-1} - 3ix^{-2} + 3x^{-3}] \exp(ix), \end{aligned} \quad (2)$$

with  $\hat{G}\mathbf{d} = G_{\alpha\beta} d_\beta$ . The Greek indices represent the Cartesian components of vectors and the summation over the repeated indices is implied.

There are two important parameters in Eq. (1). The first parameter is the polarizability of a monomer,  $\alpha_0$ , usually given by the Clausius-Mossotti relation (see, for example [11]) with the radiative correction introduced by Draine [12]

$$\alpha_0 = \frac{\alpha_{LL}}{1 - i(2k^3/3)\alpha_{LL}} \quad (3)$$

$$\alpha_{LL} = R^3 \frac{\epsilon - 1}{\epsilon + 2}, \quad (4)$$

where  $\epsilon$  is the dielectric permittivity and  $\alpha_{LL}$  is the Lorentz-Lorenz polarizability without the radiation correction.

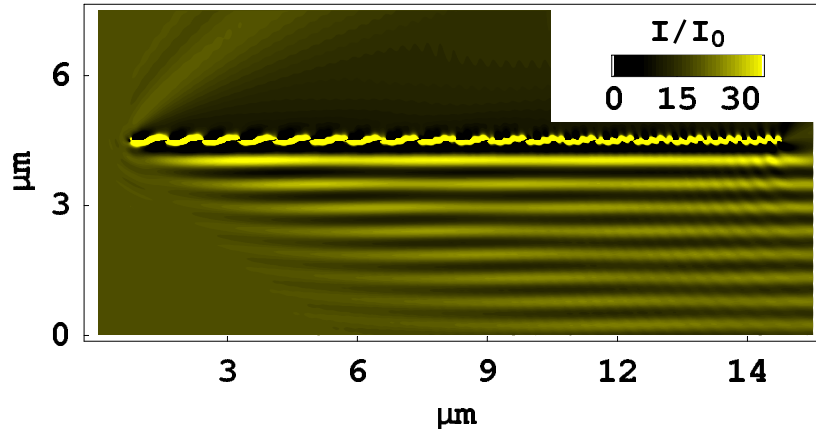


Fig. 2. Intensity enhancement distribution around silver nanowire excited by a plane electromagnetic wave [8]. The wavelength of incident light is 540 nm. The angle between the needle and the light wavevector is 30°, the wavevector and vector  $\mathbf{E}$  of the incident irradiation are in the plane of the figure

The second important parameter in the CDEs is the ratio of the radius of individual polarizable sphere  $R$  to the lattice size  $a$ . In their original work, Purcell and Pennypacker [10] proposed to choose the value for this parameter so that the total volume of the spheres is equal to the total volume of the object,

$$a/R = (4\pi/3)^{1/3} \approx 1.612 \quad (5)$$

Note that in this case two neighboring particles have to geometrically intersect since  $a/R < 2$ ; such intersection, phenomenologically, takes into account the multipolar corrections in the depolarization factor, remaining within the dipolar approximation. As shown later by Markel [13, 14], the “intersection ratio” for an infinitely long chain of spheres should slightly differ from the one given by Eq. (5) in order to give the correct depolarization factors:  $a/R \approx 1.688$ . According to Draine’s calculations [15] the value given by Eq. (5) leads to small (about 1%) error in the absorption coefficient in the quasi-static case for a spherical system. Our simulations suggest that results of simulations strongly depend on the intersection ratio  $a/R$ . In our simulations below, we choose the value of this parameter from the condition that the solution to the CDEs give the correct depolarization factor for a single nanowire.

### 3. SPP resonance in single nanowires and percolation nanowire composites

In this section, we first consider the optical properties of single nanowires. Specifically, we consider the response of a nanowire about 30 nm thick and about  $1.5 \mu\text{m}$  long illuminated by a plane wave with the vacuum wavelength of 540 nm. We model the nanowire by four parallel arrays of polarizable spheres (see Fig. 1). This 2x2 in cross-section system allows us to account for the skin-effect [8].

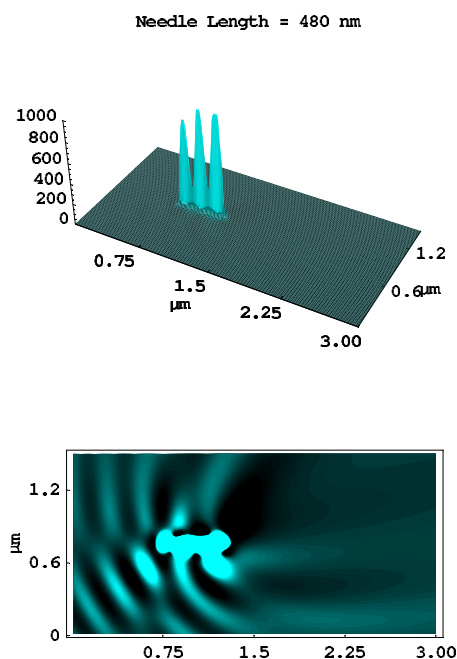


Fig. 3. Surface plasmon polariton resonance in a silver nanowire excited by a plane electromagnetic wave [8]. The intensity distribution (top panel) and simulated near-field optical microscope image (bottom panel) are shown. The wavelength of incident light is 540 nm; the angle between the nanowire and the wavevector of the incident light is  $30^\circ$ . The wavevector and  $\mathbf{E}$  vector of the incident irradiation are in the plane of the figure; the needle length is 480 nm

Results of our calculations are shown in Fig. 2. We can clearly see the interference between the incident irradiation and the surface plasmon polaritons (SPPs) excited in the nanowire. Similar interference pattern was observed in experiments [16, 17]. Note that the electromagnetic field is primarily concentrated around the wire surface, which suggests that nanowires can act as nano-waveguides.

Our simulations also show the existence of sharp SPP resonance [8] when the needle

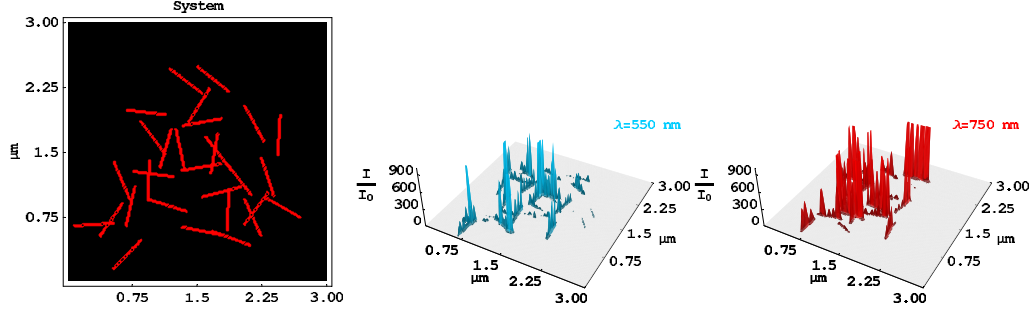


Fig. 4. Nanowire percolation Ag composite (left) and the field distribution over this composite for the incident wavelength of 550 nm (center) and 750 nm (right). In both figures the case of normal incidence with  $\mathbf{E}||x$  is considered [8]

length is an integer number of the half-wavelengths of the SPP. In resonance, the intensity of the electric field can exceed the incident field by  $10^3$ . The spatial area, where the field is concentrated is highly localized around the nanowire, and can be as small as 100 nm (Fig. 3). Note also that the SPP resonance in a single nanowire is narrow, with the width of about 50 nm.

In contrast to isolated nanowires, the spectral band covered by the SPP modes is very broad when nanowires form a percolation composite. In such composite, the nanowires are randomly distributed along the surface of a dielectric substrate, forming a thin 2D film. When the metal concentration reaches the “percolation threshold”, there is a continuous conducting path through the sample [18]. There are strong interactions between individual wires in the composite resulting in collective plasmon modes with different frequencies. At percolation, the collective SPP modes tend to be spatially localized in different parts of the film; each of these modes have different frequencies depending on the local configuration of the nanowires in the place where the modes are located. The SPP modes excited by incident radiation are concentrated in small clusters of wires which are in resonance with the frequency of light. Because of large variety in the structures of such clusters, the resonances can occur for a very broad range of frequencies. This effect is similar to localization of plasmon modes in percolation films formed by small metal nanoparticles studied earlier [19, 20]. Note that in contrast to conventional percolation films, where the percolation occurs at 50% metal filling factor, the percolation threshold for a nanowire composite is proportional to the ratio  $b_2/b_1$  and can be made arbitrary small [21], i.e., the percolation in this case, takes place at negligible metal concentrations. An example of a percolation composite and a typical field distribution over it is shown in Fig. 4.

#### 4. Effective dipole and magnetic response of the nanowire pairs

In this section we show that in the far zone the field scattered by a pair of nanowires can be approximated by the effective dipole and magnetic moments, even when the size of the pair is comparable with the wavelength  $\lambda$  of the incident light. Electric and magnetic fields at the distance  $R$  away from the nanowire pair with dimensions  $2b_1 \times d \times 2b_2$  (see Fig. 5(a)) are derived from the vector potential  $\mathbf{A}$  that for the distances  $R \gg \lambda, b_1, b_2, d$  takes the standard form  $\mathbf{A} = (e^{ikr}/cR) \int e^{-ik(\mathbf{n} \cdot \mathbf{r})} \mathbf{j}(\mathbf{r}) d\mathbf{r}$ , where  $\mathbf{j}(\mathbf{r})$  is the current density inside the nanowires and vector  $\mathbf{n}$  is the unit vector in the direction of observation. We introduce vector  $\mathbf{d}$  directed from one nanowire to another and assume that the coordinate system has its origin in the center of the system so that centers of each wires have coordinates  $\mathbf{d}/2$  and  $-\mathbf{d}/2$ , respectively. The direction of propagation of electromagnetic wave is such that the wavevector  $\mathbf{k} \parallel \mathbf{d}$  (see Fig. 5).

Then the vector potential  $\mathbf{A}$  can be written as

$$\mathbf{A} = \frac{e^{ikR}}{cR} \left[ e^{-\frac{ik}{2}(\mathbf{n} \cdot \mathbf{d})} \int_{-b_1}^{b_1} e^{-\frac{ik}{2}(\mathbf{n} \cdot \boldsymbol{\rho})} \mathbf{j}_1(\rho) d\rho + e^{\frac{ik}{2}(\mathbf{n} \cdot \mathbf{d})} \int_{-b_1}^{b_1} e^{-ik\mathbf{n} \cdot \boldsymbol{\rho}} \mathbf{j}_2(\rho) d\rho \right], \quad (6)$$

where  $\mathbf{j}_1$  and  $\mathbf{j}_2$  are the currents in the wires, and  $\rho$  is the coordinate along the wires ( $\rho \perp \mathbf{d}$ ). It is well known that the dipole component is dominating in the scattering of a thin antenna, even for the antenna size comparable with a wavelength (see, e.g., [11]). Therefore we can replace the term  $e^{-ik\mathbf{n} \cdot \boldsymbol{\rho}}$  in Eq. (6) by unity. Note that for the forward and back scattering, which is responsible for the effective properties of the medium, this term exactly equals one.

We consider the system where the distance  $d$  between the wires is much smaller than the wavelength and expand Eq. (6) in series of  $d$ ,

$$\mathbf{A} = \frac{e^{ikR}}{cR} \left[ \int_{-b_1}^{b_1} (\mathbf{j}_1 + \mathbf{j}_2) d\rho - \frac{ik}{2} (\mathbf{n} \cdot \mathbf{d}) \int_{-b_1}^{b_1} (\mathbf{j}_1 - \mathbf{j}_2) d\rho \right]. \quad (7)$$

The first term in the square brackets in Eq. (7) gives the effective dipole moment  $\mathbf{P}$  for the system of two nanowires and its contribution to the scattering can be written as  $\mathbf{A}_d = -ik(e^{ikR}/R)\mathbf{P}$ , where

$$\mathbf{P} = \int \mathbf{p}(\mathbf{r}) d\mathbf{r}, \quad (8)$$

with  $\mathbf{p}$  being the local polarization; the integration in Eq. (8) is over the volume of both wires. The second term in Eq. (7) gives the magnetic dipole and quadrupole contributions to the vector potential:

$$A_{mq} = -\frac{ike^{ikR}}{R} \left[ [\mathbf{n} \times \mathbf{M}] + \frac{\mathbf{d}}{2c} \int_{-b_1}^{b_2} (\mathbf{n} \cdot (\mathbf{j}_1 - \mathbf{j}_2)) d\rho \right], \quad (9)$$

where  $\mathbf{M}$  is the magnetic moment of the two wires,

$$\mathbf{M} = \frac{1}{2c} \int [\mathbf{j}(\mathbf{r}) \times \mathbf{r}] d\mathbf{r}, \quad (10)$$

and the integration is over the volume of the wires, as in Eq. (8).

We focus on the dipole  $\mathbf{P}$  and magnetic  $\mathbf{M}$  moments given by Eqs. (8) and (10), respectively, since they provide the main contributions to the forward and back scattering. The second term in Eq. (9) describes a quadrupole contribution; the magnetic field associated with this term is proportional to  $[\mathbf{n} \times \mathbf{k}] \int_{-b_1}^{b_1} (\mathbf{n} \cdot (\mathbf{j}_1 - \mathbf{j}_2)) d\rho$  in the far zone. This term equals zero in the direction  $\mathbf{k}$  of the incident wave (and the opposite direction) and it achieves the maximum in the direction of the wires  $\mathbf{n} \parallel \boldsymbol{\rho}$ . This ‘‘oblique’’ scattering is dumped when the coupled wires are arranged in a regular array. Yet, the oblique scattering can result in the excitation of a surface wave in a layer of the coupled wires; we do not consider this effect here.

## 5. Negative refraction in nanowire composites

In this section we consider the optical response of a particular configuration of two nanowires parallel to each other. We show that both *dielectric* and *magnetic* optical responses of such a system have strong resonances. We suggest that this specific nanowire configuration can be employed as a structure unit for a left-handed material in the

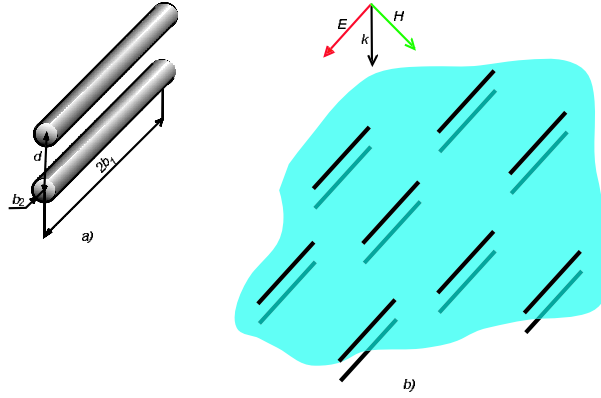


Fig. 5. Two parallel nanowires (a) and a layer of such pairs (b). A composite material based on such nanowire pairs may have the negative refraction index in the optical range [8]

near-IR and visible frequency ranges. We illustrate this idea by considering magnetic and dielectric polarization properties of a layer made of such nanowire pairs subjected to a plane electromagnetic wave incident normally onto the layer.

The proposed structure unit for a left-handed material consists of two nanowires parallel to each other (see Fig. 5). As in the previous sections, we assume that the radius of individual nanowires  $b_2$  is much smaller than the wavelength of the incident light, while the length of nanowires  $2b_1$  can be comparable with the wavelength. The distance between the wires,  $d$ , is much smaller than the wire length.

We suppose that the incident wave is polarized so that its electric component  $E$  is parallel to the axis of nanowires in the pair, whereas the magnetic component  $H$  is perpendicular to the nanowire pair (the nanowires within each pair are placed on top of each other and the pairs form a layer as shown in Fig. 5).

In this considered geometry, the electric field excites SPPs in the nanowires, which can be characterized by the *effective dipole moments*.

The magnetic field, which is perpendicular to the pair, excites a circular current in the nanowire pair. It is represented by the conduction currents inside the wires and by the displacement currents between them. Thus, the conduction current in the wires is “closed” at the ends of nanowires by the displacement currents so that there is a close current loop in each pair of nanowires. It is important that the displacement current in the optical range is large as opposed to the microwave and lower frequency ranges. Therefore, the magnetic field can effectively excite the *magnetic moments* in the nanowire pairs associated with the closed-loop currents.

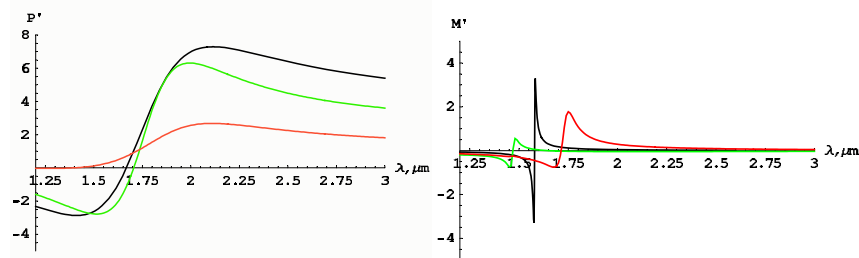


Fig. 6. Numerically simulated dielectric (left panels) and magnetic (right panels) moments for single nanowires ( $b_1 = 0.35\mu m$ ,  $b_2 = 0.05\mu m$ ) (green lines) and their pairs ( $d = 0.15\mu m$ ) (red lines) compared to the analytical Eqs. (11) (black lines). Magnetic moment of the single nanowire is multiplied by 10. The moments are normalized to the unit volume.

To illustrate the consideration above, we first numerically simulate the dielectric and magnetic moments in *single* nanowires using the DDA approach described above and compare these moments with those excited in a two-wire system (Fig. 6). For the dipole moment response in a single wire, we see the strong “antenna” resonance when the wavelength of the incident light is close to  $4b_1$ . In the two wire system this resonance becomes somewhat weaker and broader. The induced magnetic moment in a single nanowire is extremely small, as expected; we still can identify the resonance corresponding to the excitation of a circular current on the nanowire surface. This resonance is greatly enhanced in the two-wire system as seen in Fig. 6.

According to our simulations, both the dielectric and magnetic moments excited in the nanowire system are opposite to the excited field when the wavelength of the incident field is below the resonance. This means that in this frequency range a composite material based on nanowire pairs can have the negative refraction index and act like a left-handed media.

Now we compare results of our calculations with analytical formulas of Refs. [8, 21] derived for the case of needles with a high aspect ratio  $b_1/b_2$  (see Fig. 6):

$$\begin{aligned} M &= 2Hb_1^3C_2(kd)^2 \frac{\tan(gb_1) - gb_1}{(gb_1)^3} \\ P &= \frac{2}{3}b_1b_2^2f(\Delta)E\epsilon_m \frac{1}{1 + f(\Delta)\epsilon_m(b_1/b_2)^2 \ln(1 + b_1/b_2) \cos \Omega}, \end{aligned} \quad (11)$$

where  $C_2 = \frac{1}{4 \ln(d/b_2)}$  is the system capacity per unit length; the dimensionless frequency is given by  $\Omega^2 = (b_1k)^2 \frac{\ln(b_1/b_2) + ikb_1}{\ln(1 + b_1/b_2)}$ , and  $g = k\sqrt{1 + i \frac{1}{2\Delta^2 f(\Delta) \ln(d/b_2)}}$ . The function  $f(\Delta) = \frac{1-i}{\Delta} \frac{J_1[(1+i)\Delta]}{J_0[(1+i)\Delta]}$  is introduced to account for the skin effect; the parameter  $\Delta = b_2\sqrt{2\pi\sigma_m\omega}/c \gg 1$  represents the ratio of the nanowire radius and the skin depth, and  $\sigma_m$  is the bulk metal conductivity. Although the numerical results shown in Fig. 6 and the theoretical calculations presented in Fig. 7 are qualitatively similar there are also some differences.

The formulas (11) were obtained under the assumption  $b_1 \gg d \gg b_2$ , which is not exactly the case in our numerical simulations. Also, when considering the response to the electric field in derivation of Eqs. (11), we assumed that the two wires in the system interact with the electric field independently, which is indeed only a rough approximation. In accordance with this, when comparing the lines in Fig. 6, we see that the dipole response in Eqs. (11) represents better the dipole moment of an isolated nanowire rather than that for the pair. Note that the dipole response of the pair is weaker than the response of a single nanowire due to radiation losses. Furthermore, in derivation of the magnetic response in Eqs. (11), we didn't take into account the radiation decay in the magnetic response, which can significantly increase the width of the magnetic resonance, as can be seen in Fig. 6. Despite the differences, we can conclude that theoretical formulas (11) do predict qualitatively similar behavior for the electric and magnetic responses when compared with the numerical simulations and thus they can be useful in estimates of the electric and magnetic responses in metal nanowires.

We also studied numerically the induced dielectric and magnetic moments in the nanowire pair as functions of important parameters of the system. Two kinds of numerical simulations were performed along these lines. We first varied the thickness of nanowires, keeping the distance between the wires constant. Then, we varied the distance between the wires, keeping the nanowire sizes constant.

Our simulations show that the resonances become stronger for both dielectric and magnetic moments with a decrease of the nanowire thickness  $b_2$ . However, we should

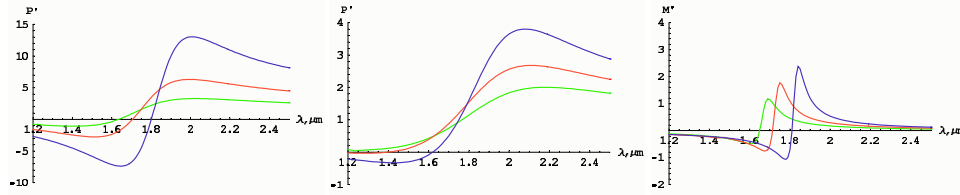


Fig. 7. Dielectric moments for individual nanowires (left) and for nanowire pairs (center) and magnetic moments for nanowire pairs as functions of wavelengths. The nanowire thickness is varied for different plots:  $b_2 = 0.035\mu\text{m}$  (blue),  $b_2 = 0.05\mu\text{m}$  (green), and  $b_2 = 0.07\mu\text{m}$  (red); for all plots,  $b_1 = 0.35\mu\text{m}$  and  $d = 0.23\mu\text{m}$ . The moments are normalized to the unit volume

note that this parameter should be kept comparable to the skin depth in the nanowire material [8] (Fig. 7).

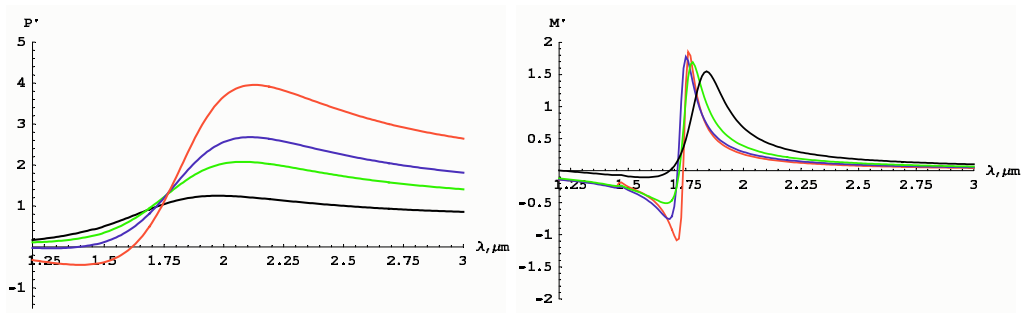


Fig. 8. Dielectric (left) and magnetic (right) moments in nanowire pairs as functions of wavelengths. The distance between the nanowires in the pairs is varied:  $d = 0.15\mu\text{m}$  (red),  $d = 0.23\mu\text{m}$  (blue),  $d = 0.3\mu\text{m}$  (green), and  $d = 0.45\mu\text{m}$  (black)); for all plots,  $b_1 = 0.35\mu\text{m}$  and  $b_2 = 0.05\mu\text{m}$ . The moments are normalized to the unit volume

When we gradually increase the separation between the nanowires (i.e., increase parameter  $d$ ), the interaction between the wires becomes smaller and the radiative losses in the system increase. As a result, both the dielectric and magnetic resonances become weaker, resulting in a decreased region for the “negative responses”; the magnetic resonance practically vanishes at larger distances, when the interaction between the wires is negligible (Fig. 8). The dielectric moment, however, starts to grow again after some critical distance between the wires have been achieved, regaining its value for the isolated nanowire (not shown). We didn’t vary the length of nanowires since as mentioned above, the nanowire length should be closed to the half of the resonant wavelength,  $\lambda_{res} \approx 4b_1$ , for the efficient excitation of SPP in nanowires. We also note that the radiative losses could be significant in the coupled nanowire systems. Our simulations suggest that losses increase as we increase the distance between the wires  $d$  or the thickness of the wire  $b_2$  (Fig. 9). With a decrease of the wire thickness, the effect becomes stronger and losses smaller; we expect that the effect is particularly strong at the wire thickness close to the skin-depth (20 nm).

We note that various composites based on metal nanowires can be developed that have the macroscopic negative refraction and act as left-handed materials. For example, such left-handed materials can be based on a multi-layer structure, with each layer consisting of pairs of the parallel nanowires, as the one shown in Fig. 5. Even a single layer of nanowire pairs can show unusual optical properties related to the negative refraction. It is interesting to note that instead of using pairs of real nanowires one can prepare a layer of single nanowires and place it above a metal surface so that

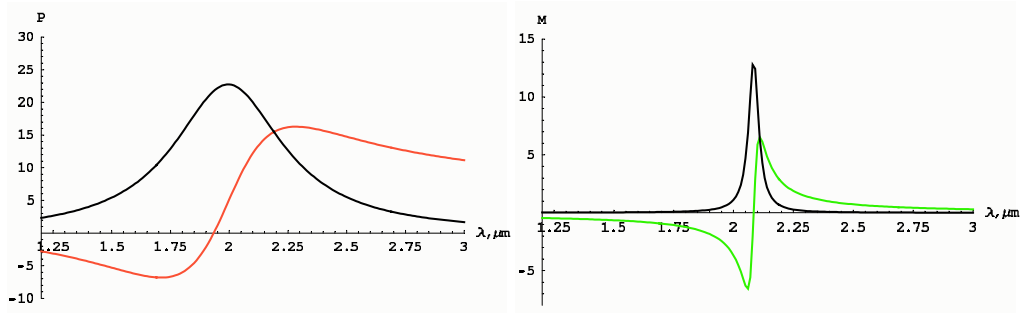


Fig. 9. Real (colored) and imaginary (black) parts of dielectric (left) and magnetic (right) moments in nanowire pair as functions of wavelengths. The system parameters:  $d = 0.075\mu\text{m}$ ,  $b_1 = 0.35\mu\text{m}$  and  $b_2 = 0.025\mu\text{m}$ . The moments are normalized to the unit volume

when irradiated by light the “image” nanowires are induced inside the metal, for every real wire. Then, by placing a dielectric spacer of different thickness between the layer of the nanowires and the metal surface, one can control the separation between the wires in the pairs, formed by the real (upper) and image (lower) nanowires. We also note that a 3D random composite of nanowires combined into pairs can also have the macroscopic negative refraction. Finally, composite materials (including random ones) formed by single (rather than pairs of) nanowires may also show the negative refraction, under some conditions; however, the effect in this case is expected to be smaller. Thus, there are different ways of fabricating nanowire composites that can act as left-handed materials in the optical range.

## 6. Conclusions

In this paper we numerically study the optical properties of single nanowires, their pairs, and nanowire composites. We demonstrate the existence of surface plasmon polariton modes in such nanowires. We also show that the enhancement for the local fields can be very large when the incident radiation is in resonance with the surface plasmon polaritons (SPPs) in the wires. We find that in percolation composites of nanowires there is a broad band of resonant modes related to spatially localized SPP modes. Finally, we show that composite materials based on nanowires may possess a negative refractive index and act as left-handed materials in the optical range of the spectrum.

## Acknowledgements

The work was supported in part by NSF-NIRT grant 0210445-ECS, NASA grant NCC-1-01049, and by NSF grant DMR-0121814.